Journal of Materials Science: Materials in Electronics
https://doi.org/10.1007/s10854-020-03927-1

Microwave dielectric properties of novel $(1-x)MgTiO_3$–$xCa_{0.5}Sr_{0.5}TiO_3$ ceramics

Chuying Chen[1] · Zhijian Peng[1] · Luzhi Xie[1] · Ke Bi[2] · Xiuli Fu[2]

Received: 16 April 2020 / Accepted: 1 July 2020
© Springer Science+Business Media, LLC, part of Springer Nature 2020

Abstract
In this work, the microstructure and microwave dielectric properties of novel $(1-x)MgTiO_3$–$xCa_{0.5}Sr_{0.5}TiO_3$ ($x=0.035$–0.045) ceramics were investigated. The samples were prepared via the solid-state sintering method using the pre-synthesized ultrafine $MgTiO_3$ and $(Ca_{0.5}Sr_{0.5})TiO_3$ powders by molten-salt reaction. As the x value increases from 0.035 to 0.045, the quality factor ($Q{\cdot}f$) of the samples presents an increase first and then a decrease, reaching the maximum of 70,000 with $x=0.0375$. The dielectric constant (ε_r) increases monotonously with the increase of x, which is 20.96 when $x=0.0045$. The temperature coefficient of resonant frequency (τ_f) progressively increases with increasing content of $Ca_{0.5}Sr_{0.5}TiO_3$. When $x=0.004$, the obtained $0.96MgTiO_3$–$0.04Ca_{0.5}Sr_{0.5}TiO_3$ ceramics sintered at 1275 °C for 4 h display excellent microwave dielectric properties with an ε_r value of about 20.57, a relatively high $Q{\cdot}f$ value of roughly 58,000 GHz, and a near-zero τ_f value of approximately − 1.16 ppm/°C. Such ceramics might be a good candidate for high-performance microwave dielectric devices.

1 Introduction

In global wireless communication system, various microwave dielectric components have been rapidly developed in the last decades, in which microwave dielectric materials play a key role with massive employments [1–5]. In order to meet the demands for high-performance microwave devices, there are three major features that excellent dielectric materials should possess: an appropriate dielectric constant (ε_r), high quality factor ($Q{\cdot}f$) and near-zero temperature coefficient of resonant frequency (τ_f) [6, 7]. A higher ε_r value would facilitate the miniaturization of devices, high $Q{\cdot}f$ enables a low loss, and near-zero τ_f provides a high stability at varied application temperatures [8].

Among all the low-loss materials with a medium dielectric constant, ilmenite-structured magnesium titanate ($MgTiO_3$) is one of the well-known candidates in industry [9, 10]. Because of their low dielectric loss, $MgTiO_3$ ceramics have been widely applied in dielectric components such as phase shifters, tunable filters, antennas, and stabilizers of frequency oscillation for the communications at microwave frequency [11, 12]. Generally, $MgTiO_3$ ceramics possess good dielectric performances with an ε_r value of about 17 and $Q{\cdot}f$ of roughly 160,000 GHz (at 7 GHz) [13]. However, the τ_f value of pure $MgTiO_3$ ceramics is roughly − 50 ppm/°C, which is not appropriate for such devices. To obtain dielectric materials with a near-zero τ_f value, the normally adopted approaches are to combine two or more materials of opposite τ_f values to form a solid solution or mixed phases [14–16]. Therefore, the compositing of $MgTiO_3$ with other compounds of a positive τ_f value is considered as the most feasible way to produce the desired high-performance $MgTiO_3$-based microwave dielectric materials with a near-zero τ_f value. In the literature, the perovskite-structured $CaTiO_3$ ($\varepsilon_r=170$, $Q{\cdot}f=3600$ GHz and $\tau_f=800$ ppm/°C) and $SrTiO_3$ ($\varepsilon_r=290$, $Q{\cdot}f=4800$ GHz and $\tau_f=1700$ ppm/°C) are generally introduced into microwave dielectric ceramics on account of their high positive τ_f values [17–20]. For the preparation of $MgTiO_3$-based microwave dielectric ceramics, Huang et al. [21] indicated that with a ratio of Mg:Ca = 95:5, the obtained $0.95MgTiO_3$–$0.05CaTiO_3$

✉ Zhijian Peng
pengzhijian@cugb.edu.cn

✉ Xiuli Fu
xiulifu@bupt.edu.cn

[1] School of Science, China University of Geosciences, Beijing 100083, People's Republic of China

[2] School of Science, Beijing University of Posts and Telecommunications, Beijing 100876, People's Republic of China

Published online: 09 July 2020

ceramics possessed a near-zero τ_f value with $\varepsilon_r = 20$–21 and $Q{\cdot}f = \sim 56{,}000$ GHz (at 7 GHz). Also in 2004, it was reported that $0.964MgTiO_3$–$0.036SrTiO_3$ ceramics exhibited an excellent dielectric performance with $\varepsilon_r = 20.76$, $Q{\cdot}f = 71{,}000$ GHz, and $\tau_f = -1.27$ ppm/°C [22]. Owing to the similar perovskite structure between $SrTiO_3$ and $CaTiO_3$, it was indicated that $Ca_xSr_{1-x}TiO_3$ solid solution such as $Ca_{0.8}Sr_{0.2}TiO_3$ and $Ca_{0.5}Sr_{0.5}TiO_3$ would also show a good dielectric feature [23]. So later in the work of Pan et al. [24], $Ca_{0.8}Sr_{0.2}TiO_3$ ($\varepsilon_r = 180$, $Q{\cdot}f = 8300$ GHz and $\tau_f = 990$ ppm/°C) was added into $MgTiO_3$ to prepare a series of $(1-x)MgTiO_3$–$xCa_{0.8}Sr_{0.2}TiO_3$ ceramics, optimizing that $0.94MgTiO_3$–$0.06Ca_{0.8}Sr_{0.2}TiO_3$ ceramics possessed an excellent combination of microwave dielectric properties: $\varepsilon_r = \sim 21.9$, $Q{\cdot}f = \sim 128{,}000$ GHz, and $\tau_f = \sim 0.7$ ppm/°C. And Zhang et al. [25] revealed that after the doping of $Ca_{0.8}Sr_{0.2}TiO_3$, the obtained $0.78MgTiO_3$–$0.22Ca_{0.8}Sr_{0.2}TiO_3$ ceramics could provide a combination of dielectric properties of $\varepsilon_r = 20.25$, $Q{\cdot}f = 74{,}200$ GHz, and $\tau_f = -1.28$ ppm/°C. Moreover, it is known that $Ca_{0.5}Sr_{0.5}TiO_3$ ($\varepsilon_r = 240$ and $Q{\cdot}f = 4100$ GHz) possesses a higher ε_r value than $Ca_{0.8}Sr_{0.2}TiO_3$ [23], and its temperature coefficient of dielectric constant (τ_ε) decreases with the increase of the ε_r value [26]. Since $\tau_f \approx -(1/2)\tau_\varepsilon$, the τ_f value of a dielectric material would increase as ε_r increases [26–28]. In other words, $Ca_{0.5}Sr_{0.5}TiO_3$ should also have a higher τ_f value than $Ca_{0.8}Sr_{0.2}TiO_3$. Therefore, $Ca_{0.5}Sr_{0.5}TiO_3$ would be a better choice to combine with $MgTiO_3$ to produce the desired high-performance microwave dielectric materials with a near-zero τ_f value. Through doping less amount of secondary $Ca_{0.5}Sr_{0.5}TiO_3$ phase, such combination is expected to obtain a $MgTiO_3$-based dielectric ceramic composite with a near-zero τ_f, high ε_r, and even high $Q{\cdot}f$ value. However, to the best of our knowledge, no work about the preparation of $Ca_{0.5}Sr_{0.5}TiO_3$-doped $MgTiO_3$ microwave dielectric ceramics has been reported.

In this work, different amounts of $Ca_{0.5}Sr_{0.5}TiO_3$ were designed to add into $MgTiO_3$ matrix to prepare a series of composite ceramics, which had a nominal composition of $(1-x)MgTiO_3$–$xCa_{0.5}Sr_{0.5}TiO_3$ ($(1-x)$MT–xCST, where $x = 0.035$–0.045 with a step of 0.025). The samples were prepared via the solid-state sintering method using the presynthesized ultrafine $MgTiO_3$ and $(Ca_{0.5}Sr_{0.5})TiO_3$ powders by molten-salt reaction. The molten-salt synthesis was adopted because it could prepare the ultrafine powders to promote the sintering of the final composite ceramics [29]. The microstructure and microwave dielectric properties of the obtained ceramics were systematically investigated. As expected, temperature-stable microwave dielectric ceramics with high $Q{\cdot}f$ and moderate ε_r values were obtained through adjusting the value of x. Such ceramics might be a good candidate for high-performance microwave dielectric devices.

2 Experimental procedure

2.1 Samples preparation

$MgTiO_3$ and $Ca_{0.5}Sr_{0.5}TiO_3$ ultrafine powders were first separately prepared by a modified molten-salt synthesis method [29] from high-purity raw powders of $MgCl_2{\cdot}6H_2O$ (> 99.0%), $SrCl_2{\cdot}6H_2O$ (> 99.0%), $CaCl_2$ (> 99.0%), NaOH (> 96.0%), KOH (> 99.0%), and TiO_2 (> 99.0%). All the chemicals were bought from Sinopharm Group Co. Ltd., which were used as received. During typical process, the raw powders in stoichiometry were accurately weighed and mixed in distilled water for 24 h by rotational ball milling with highly wear-resistant ZrO_2 balls as the grinding media. Then the slurries were dried at 120 °C for 10 h in air, and the resultant powder chunks were calcined in a Muffle furnace for 3 h at 900 °C for $MgTiO_3$ and 1200 °C for $Ca_{0.5}Sr_{0.5}TiO_3$, respectively. After calcination, the resultant powder chunks were ground and re-milled by rotational ball milling for 12 h. During the milling, the emulsions were cleaned by centrifuging with distilled water for several times and then the collected powders were dried again at 120 °C for 12 h.

Afterwards, the acquired powders were weighed and mixed in the designed composition $(1-x)$MT–xCST, where $x = 0.035$, 0.0375, 0.04, 0.0425, and 0.045, respectively. During the mixing, the powders were milled in distilled water for 24 h with high-resistance ZrO_2 balls as the grinding media and 10 wt% PVA as the binder. After milling, the slurries were dried again at 120 °C, and the resultant powder chunks were ground and sieved into fine powders. Then the obtained powders were pressed into pellets with a diameter of 12 mm and thickness of 6 mm under a pressure of 6 MPa. Finally, the pellets were sintered at the optimal temperature of 1275 °C for 4 h at a heating rate of 2 °C/min.

2.2 Samples characterization

The crystalline phases of the sintered samples were identified by X-ray diffraction (XRD, D/max-RB, Japan; Cu Kα, $\lambda = 1.5418$ Å) in a continuous mode at a scan speed of 4°/min. The microstructures were observed by using a scanning electron microscope (SEM, SU8020, Hitachi, Japan). An energy dispersive X-ray (EDX) spectroscope attached to the SEM was applied to investigate the elemental compositions of the samples. The apparent densities were measured based on the Archimedean principle (international standard ISO18754). The relative densities were defined as the percentage of the measured apparent density to the calculated theoretical density on the basis of mixture

rule. The microwave dielectric properties of the samples were measured on a vector network analyzer (Keysight E5063A, America) in the frequency range of 6–9 GHz. The dielectric constant was obtained by the Hakki–Coleman method, which was modified by the Courtney method [30]. The unload Q values were evaluated by the cavity method in the TE_{011} mode, and the τ_f values were calculated by the following equation [31]:

$$\tau_f = \frac{f_2 - f_1}{f_1(T_2 - T_1)} \quad (1)$$

where f_1 and f_2 represent the $TE_{01\sigma}$ resonant frequency of the samples at 25 and 85 °C, respectively.

3 Results and discussion

3.1 Phase composition and microstructure

In this work, all the $(1-x)$MT–xCST ($x = 0.035$–0.045) specimens were sintered at the optimal temperature of 1275 °C (the lowest temperature to obtain dense 0.955MT–0.045CST sample) for 4 h to exclude the impact of sintering. Figure 1 shows the XRD patterns of the $(1-x)$MT–xCST ceramics fabricated with x from 0.035 to 0.045. The results reveal that all the samples are a composite of a main ilmenite $MgTiO_3$ phase and a minor perovskite $Ca_{0.5}Sr_{0.5}TiO_3$ phase as designed. The formation of such composites could be attributed to the different phase structures between $MgTiO_3$ and $Ca_{0.5}Sr_{0.5}TiO_3$ together with the big ionic radius discrepancy between Mg^{2+} (0.72 Å), Ca^{2+} (1.00 Å), and Sr^{2+} (1.44 Å) ions in the ceramics. Therefore, all the obtained $(1-x)$MT–xCST ceramics are basically a simple solid solution of $MgTiO_3$ and $Ca_{0.5}Sr_{0.5}TiO_3$.

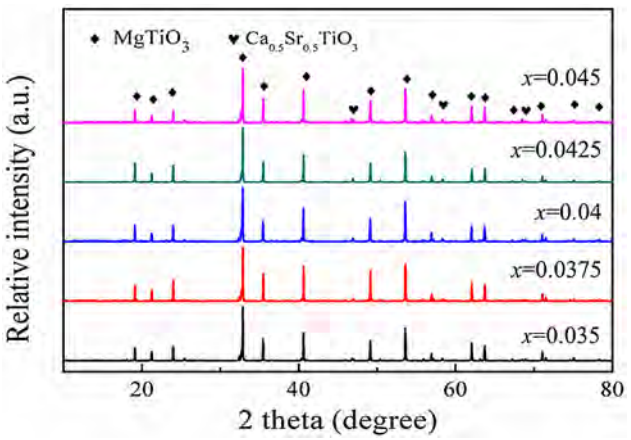

Fig. 1 XRD patterns of the obtained $(1-x)$MT–xCST ceramics

Figure 2 presents the typical second-electron SEM micrographs of the obtained $(1-x)$MT–xCST ceramics ($x = 0.035$–0.045). As is seen, the grains of the main $MgTiO_3$ phase in all the samples present a normal distribution (see Fig. 2a–e), and its average size decreases with increasing value of x, which is 5.73, 5.53, 5.35, 4.89, and 4.68 μm when x equals to 0.035, 0.0375, 0.04, 0.0425, and 0.045, respectively (see Fig. 2f). Owing to the presence of $Ca_{0.5}Sr_{0.5}TiO_3$ solid solution phase (the small particles on the big grains) in the samples, the movement of the $MgTiO_3$ grain boundary would be impeded and the re-union of $MgTiO_3$ phase became difficult. Therefore, by increasing the addition amount of $Ca_{0.5}Sr_{0.5}TiO_3$, the grain boundary of $MgTiO_3$ phase was pinned by the $Ca_{0.5}Sr_{0.5}TiO_3$ particles, which would finally result in smaller $MgTiO_3$ grains. Moreover, all the samples are quite dense. Comparatively, after the addition of $Ca_{0.5}Sr_{0.5}TiO_3$, the samples first became a little denser due to the moderate decrease in grain size of matrix $MgTiO_3$ phase, the promotion effect on sintering via solid solution and the filling effect of the small $Ca_{0.5}Sr_{0.5}TiO_3$ grains into the pores constructed by the main, big $MgTiO_3$ grains, but with more $Ca_{0.5}Sr_{0.5}TiO_3$, the sample would present a less dense structure with more pores because of the increasing pinning effect of $Ca_{0.5}Sr_{0.5}TiO_3$ on the movement of main $MgTiO_3$ phase, which will hinder the sintering of the samples.

In order to clarify the distribution of the $Ca_{0.5}Sr_{0.5}TiO_3$ solid solution phase, back-scattering electron imaging was carried out. Typical micrograph on the polished surface of the sample 0.955MT–0.045CST is presented in Fig. 3. It is seen that there are two domains on the micrograph: bright white (α) and dark gray (β), indicating two kinds of grains. According to the different sizes of the two domains, it can be deduced that the bigger ones are the matrix $MgTiO_3$ grains, while the smaller ones are the added $Ca_{0.5}Sr_{0.5}TiO_3$ particles.

EDX technique was also used to distinguish each kind of grain in the specimen. Table 1 presents the elemental contents of two kinds of grains as exhibited in Fig. 3. It was revealed that from the obtained $(1-x)$MT–xCST ceramics, O, Ti, Mg, Ca, and Sr atoms could be detected. However, on the bright white domain (α grain), there are O, Ti, Ca, and Sr atoms almost without Mg, indicating that it should be a $Ca_{0.5}Sr_{0.5}TiO_3$ particle. Meanwhile, on the dark gray domain (β grain), only O, Ti, and Mg atoms were detected, revealing that such domain is attributed to the $MgTiO_3$ grain. All these results indicate that the obtained $(1-x)$MT–xCST ceramics are a solid solution of $MgTiO_3$ and $Ca_{0.5}Sr_{0.5}TiO_3$. On combination with the XRD results, it can be confirmed that such type of solid solution would not change the phase composition of the resultant composites. In addition, it can also be seen from Fig. 3 that most of the $Ca_{0.5}Sr_{0.5}TiO_3$ grains segregate into the triangular grain boundaries of $MgTiO_3$

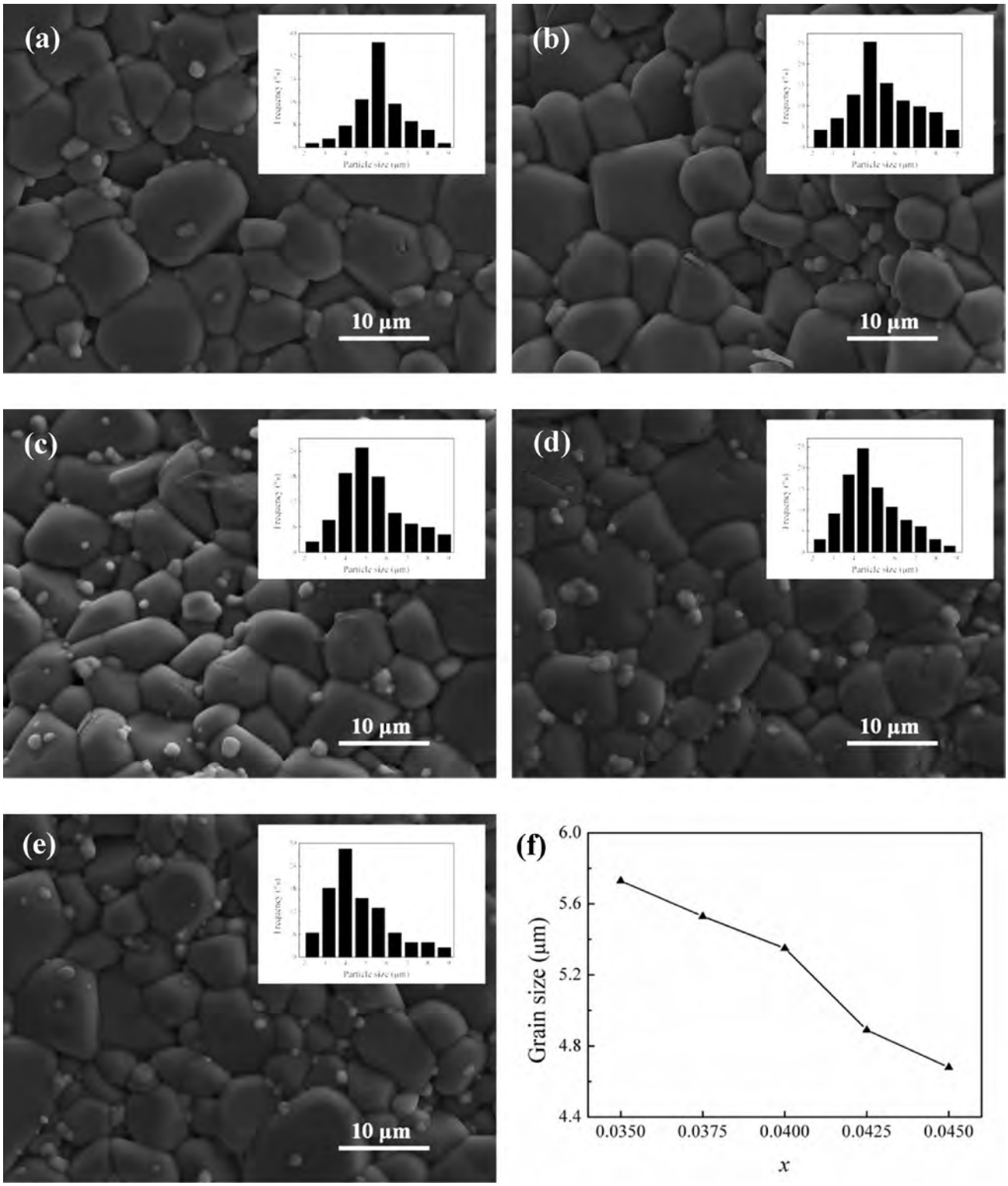

Fig. 2 Typical second-electron SEM micrographs on the polished surface of the obtained $(1-x)$MT–xCST specimens: **a** $x=0.035$, **b** $x=0.0375$, **c** $x=0.04$, **d** $x=0.0425$, and **e** $x=0.045$. Each inset exhibits the grain size distribution of the main $MgTiO_3$ phase in the specimens. **f** Relationship between x and grain size of $MgTiO_3$

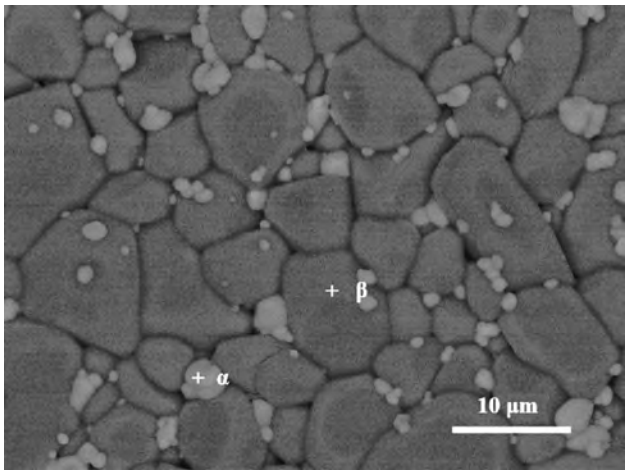

Fig. 3 Back-scattering electron image on the polished surface of the typical sample 0.955MT–0.045CST

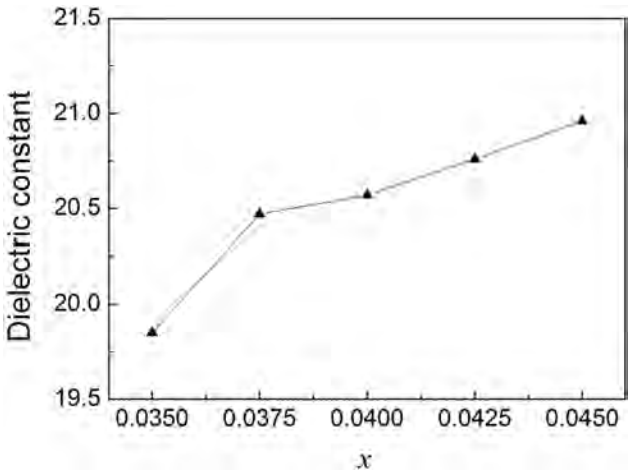

Fig. 5 The ε_r value of the obtained $(1-x)$MT–xCST ceramics ($x=0.035$–0.045)

Table 1 Elemental contents measured by EDX analysis of grains α and β as shown in Fig. 3

Elements	O (at.%)	Ti (at.%)	Mg (at.%)	Ca (at.%)	Sr (at.%)
Grain α	64.33	18.71	–	7.30	9.66
Grain β	62.06	18.6	19.27	–	–

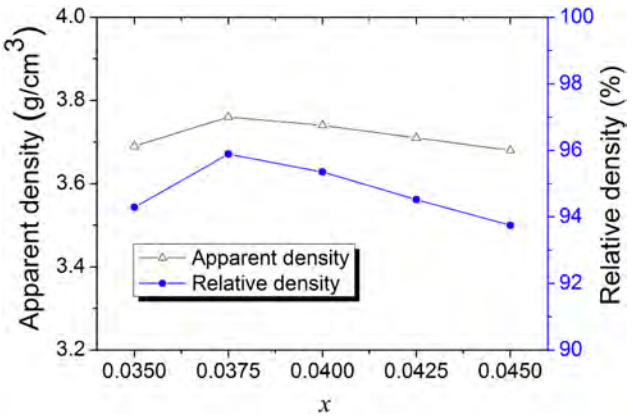

Fig. 4 Apparent density and relative density of the $(1-x)$MT–xCST ($x=0.035$–0.045) specimens

grains and less amount of $Ca_{0.5}Sr_{0.5}TiO_3$ grains are on the surface of $MgTiO_3$ grains.

Figure 4 illustrates the relationship between x, apparent density, and relative density. As can be seen, after the addition of increasing amount of $Ca_{0.5}Sr_{0.5}TiO_3$, the apparent density and relative density of the obtained $(1-x)$MT–xCST ceramics increase initially and decrease thereafter, presenting a maximum of 3.76 g/cm^3 and 95.89%, respectively, when $x=0.0375$, which is consistent with the observation by SEM imaging. The increase in the densification of the obtained samples with little amount of $Ca_{0.5}Sr_{0.5}TiO_3$ should be ascribed to the following factors: (i) the moderate decrease in grain size of matrix $MgTiO_3$ phase, which is beneficial for extruding gases in the samples; (ii) the promotion effect on sintering via solid solution, which possibly acts as liquid to aid the sintering; and (iii) the filling effect of the small $Ca_{0.5}Sr_{0.5}TiO_3$ grains into the pores constructed by the main, big $MgTiO_3$ grains (see Fig. 3). But with excessive $Ca_{0.5}Sr_{0.5}TiO_3$, the movement of $MgTiO_3$ grains would be seriously impeded due to the pinning effect of $Ca_{0.5}Sr_{0.5}TiO_3$ grains, and the sintering ability of the samples would, thus, decrease, finally resulting in a decreased densification of the samples.

3.2 Microwave dielectric properties

The ε_r value of the obtained $(1-x)$MT–xCST ceramics ($x=0.035$–0.045) is displayed in Fig. 5. It is seen that with increasing x, the ε_r value of the present samples monotonously increases, reaching 20.96 when $x=0.045$ (the maximum in the designed range of x). As is well known, ε_r represents the polarization capacity of microwave dielectric ceramics. Generally speaking, the ε_r value of a microwave dielectric composite is significantly dependent upon the secondary phase in the sample and its relative density (sample densification) [32]. For a microwave dielectric ceramic composite with two phases, its ε_r value can be estimated by using the following equation proposed by Kim [33, 34],

$$\ln \varepsilon_r = V_1 \ln \varepsilon_{r1} + V_2 \ln \varepsilon_{r2} \quad (2)$$

where ε_r represents the dielectric constant of the ceramic composite, V_1 and V_2 are, respectively, the volume fraction

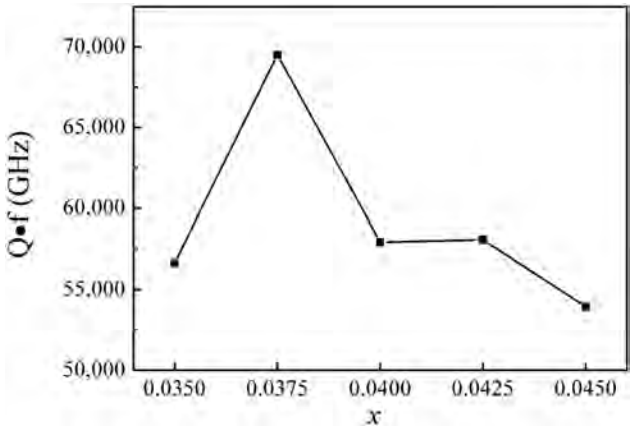

Fig. 6 The $Q{\cdot}f$ value of the obtained $(1-x)$MT–xCST ceramics ($x=0.035$–0.045)

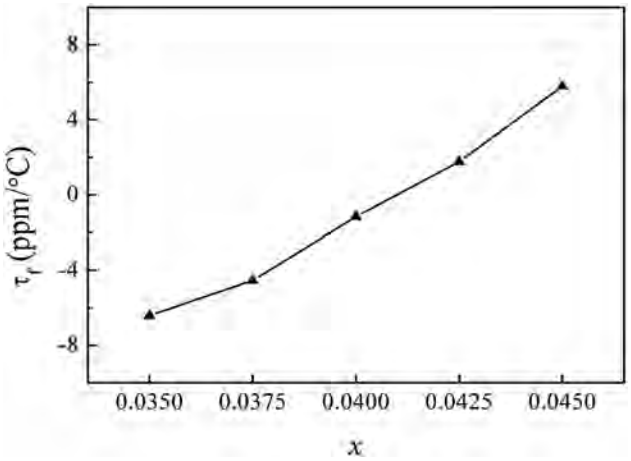

Fig. 7 The τ_f value of the obtained $(1-x)$MT–xCST ceramics ($x=0.035$–0.045)

of the constituent phases, and ε_{r1} and ε_{r2} represent the dielectric constant of the constituent phases, respectively. In this work, the additive $Ca_{0.5}Sr_{0.5}TiO_3$ has much higher ε_r ($\varepsilon_r=240$) than the matrix $MgTiO_3$ ($\varepsilon_r=17$). According to Eq. (2), with the increase of x, the ε_r value of the obtained $(1-x)$MT–xCST ceramics would increase. Moreover, when $x<0.4$, as shown in Fig. 4, the increased densification of the samples would also contribute to the increase of ε_r value. It should be noted that although the relative density of the samples decreases with excessive amount of $Ca_{0.5}Sr_{0.5}TiO_3$, the resultant negative effect on the ε_r value is less than the positive effect produced by the addition of $Ca_{0.5}Sr_{0.5}TiO_3$. Therefore, the ε_r value keeps increasing with the addition of $Ca_{0.5}Sr_{0.5}TiO_3$ for the present samples.

Figure 6 presents the $Q{\cdot}f$ value of the obtained $(1-x)$MT–xCST ceramics ($x=0.035$–0.045). As is seen, with increasing x, the $Q{\cdot}f$ value of the samples rises up first and drops down later, presenting a maximum of 70,000 when $x=0.0375$. The $Q{\cdot}f$ value is an important standard for the application of microwave components under the working frequencies since a high $Q{\cdot}f$ value implies a low dielectric loss. Generally speaking, the porosity and grain size are the two main factors which affect the dielectric loss of microwave dielectric ceramics [35, 36]. For the present $(1-x)$MT–xCST ceramics, with increasing value of x, their relative density increases initially ($x\leq0.0375$), indicating a decrease of porosity. Correspondingly, the $Q{\cdot}f$ value of the samples increases. When $x>0.0375$, the porosity of the samples increases, thus resulting in the decrease of the $Q{\cdot}f$ values. In addition, as displayed in Fig. 2f, the grain size of the obtained $(1-x)$MT–xCST ceramics exhibits a decreasing tendency with increasing value of x. The decreased grain size would lead to an increased number of grain boundaries, which would give rise to the increase of dielectric loss. Resultantly, the $Q{\cdot}f$ value of the samples would decrease. Due to the two opposite factors, a maximum $Q{\cdot}f$ value of 70,000 GHz was reached for the 0.9625 $MgTiO_3$–0.0375 $Ca_{0.5}Sr_{0.5}TiO_3$ ceramics.

Figure 7 displays the τ_f value of the obtained $(1-x)$MT–xCST ($x=0.035$–0.045) ceramics. In this work, the τ_f values were measured at 6–9 GHz in the temperature range from 25 to 85 °C. It is seen that the τ_f value of the samples varies from − 6.41 to + 5.80 ppm/°C with increasing value of x. Since the τ_f curve would go through zero point, it indicates that a ceramic composite with $\tau_f=0$ could be obtained by appropriately adjusting the x value. Generally speaking, the τ_f value of microwave dielectric materials is related to the composition or phases existing in the samples. The τ_f value of the present composite ceramics can be estimated by the following mixing rule [37],

$$\tau_f = V_1\tau_{f1} + V_2\tau_{f2} \quad (3)$$

in which V_1 and V_2 are, respectively, the volume fraction of the constituent phases, and τ_{f1} and τ_{f2} are the temperature coefficients of resonant frequency of the constituent phases, respectively. For the present $(1-x)$MT–xCST system, a sample with a near-zero τ_f value of − 1.16 ppm/°C would be obtained when $x=0.04$, which needs a relatively low content of secondary phase in the sample to reach the goal compared with the similar ceramic composites reported in the literature (see Table 2).

4 Conclusions

Novel $(1-x)MgTiO_3$–$xCa_{0.5}Sr_{0.5}TiO_3$ ($x=0.035$–0.045) composite ceramics were prepared via the solid-state sintering method using the pre-synthesized ultrafine $MgTiO_3$ and $(Ca_{0.5}Sr_{0.5})TiO_3$ powders by molten-salt reaction. The microstructures and microwave dielectric properties of the

Table 2 Comparison on modulating the τ_f values of $MgTiO_3$ systems

Compositions	Sintering parameters	$Q{\cdot}f$ (GHz)	τ_f (ppm/°C)	Refs
$0.95MgTiO_3$–$0.05CaTiO_3$	1400 °C, 3 h	56,000	0	[21]
$0.964MgTiO_3$–$0.036SrTiO_3$	1270 °C, 2 h	71,000	− 1.27	[22]
$0.94MgTiO_3$–$0.06Ca_{0.8}Sr_{0.2}TiO_3$	1300 °C, 4 h	128,000	0.7	[24]
$0.78MgTiO_3$–$0.22Ca_{0.8}Sr_{0.2}TiO_3$	1300 °C, 4 h	74,200	− 1.28	[25]
$0.96MgTiO_3$–$0.04Ca_{0.5}Sr_{0.5}TiO_3$	1275 °C, 4 h	58,000	− 1.16	This work

obtained samples were investigated. All the obtained composite ceramics consist of a main ilmenite $MgTiO_3$ phase and a minor perovskite $Ca_{0.5}Sr_{0.5}TiO_3$ phase. The addition of $Ca_{0.5}Sr_{0.5}TiO_3$ would lead to a decreased grain size of the $MgTiO_3$ phase in the samples. The densification of the samples increased first and decreased later as the x value increased from 0.035 to 0.045. When $x = 0.04$, the $0.96MgTiO_3$–$0.04(Ca_{0.5}Sr_{0.5})TiO_3$ ceramics sintered at 1275 °C for 4 h have excellent microwave dielectric properties of $\varepsilon_r = 20.57$, $Q{\cdot}f = 58{,}000$ GHz, and $\tau_f = -1.16$ ppm/°C.

Acknowledgements The authors would like to thank the financial support for this work from the National Natural Science Foundation of China (Grant Nos. 11674035 and 61274015) and the Fundamental Research Funds for the Central Universities.

References

1. J. Guo, A.L. Baker, H.Z. Guo, M. Lanagan, C.A. Randall, Cold sintering process: a new era for ceramic packaging and microwave device development. J. Am. Ceram. Soc. **100**, 669–677 (2017)
2. M.T. Sebastian, R. Ubic, H. Jantunen, Low-loss dielectric ceramic materials and their properties. Int. Mater. Rev. **60**, 392–412 (2015)
3. C.H. Hsu, C.J. Huang, Preparation, structural and microwave dielectric properties of $CaLa_4(Zr_xTi_{1-x})_4O_{15}$ ceramics. J. Alloys Compd. **587**, 45–49 (2014)
4. C.L. Huang, J.Y. Chen, C.C. Liang, Dielectric properties and mixture behavior of $Mg_4Nb_2O_9$-$SrTiO_3$ ceramic system at microwave frequency. J. Alloys Compd. **478**, 554–558 (2009)
5. S. Sahoo, Enhanced time response and temperature sensing behavior of thermistor using Zn-doped $CaTiO_3$ nanoparticles. J. Adv. Ceram. **7**, 99–108 (2018)
6. A. Templeton, X.R. Wang, S.J. Penn, S.J. Webb, L.F. Cohen, N.M. Alford, Microwave dielectric loss of titanium oxide. J. Am. Ceram. Soc. **83**, 95–100 (2000)
7. F. Qin, S. Zhang, R.Z. Zuo, Ultralow-loss and thermally stable $Li_4MgSn_{2-1.25x}Nb_xO_7$ microwave dielectric ceramics. J. Mater. Sci. (2020). https://doi.org/10.1007/s10854-020-03121-3
8. M.J. Wu, Y.C. Zhang, M.Q. Xiang, Synthesis, characterization and dielectric properties of a novel temperature stable $(1-x)CoTiNb_2O_{8-x}$-$ZnNb_2O_6$ ceramic. J. Adv. Ceram. **8**, 228–237 (2019)
9. H.J. Jo, E.S. Kim, Dependence of microwave dielectric properties on the complex substitution for Ti-site of $MgTiO_3$ ceramics. Ceram. Int. **43**, S326–S333 (2017)
10. L. Nikzad, H. Majidian, S. Ghofrani, T. Ebadzadeh, Sintering behavior and microwave dielectric properties of $MgTiO_3$ obtained from coprecipitation method with additives. Int. J. Appl. Ceram. Technol. **15**, 569–574 (2018)
11. U. Ullah, W.F.F.W. Ali, M.F. Ain, N.M. Mahyuddin, Z.A. Ahmad, Design of a novel dielectric resonator antenna using $MgTiO_3$-$CoTiO_3$ for wideband applications. Mater. Des. **85**, 396–403 (2015)
12. Y.C. Chen, S.M. Tsao, C.S. Lin, S.C. Wang, Y.H. Chien, Microwave dielectric properties of $0.95MgTiO_3$-$0.05CaTiO_3$ for application in dielectric resonator antenna. J. Alloys Compd. **471**, 347–351 (2009)
13. K. Wakino, Recent development of dielectric resonator materials and filters in Japan. Ferroelectrics **91**, 69–86 (1989)
14. D.Y. Gui, C.H. Wang, W.J. Zhu, C.M. Meng, Phase controlled Raman modes and dielectric properties in $(1-x)MgTiO_{3-x}(Mg_4Ta_2O_9)_{1/3}$. J. Alloys Compd. **730**, 434–440 (2018)
15. L.X. Li, S. Li, T. Tian, X.S. Lyu, J. Ye, H. Sun, Microwave dielectric properties of $(1-x)MgTiO_3-x(Ca_{0.6}Na_{0.2}Sm_{0.2})TiO_3$ ceramic system. J. Mater. Sci. **27**, 1286–1292 (2016)
16. Y.C. Liou, Y.C. Wu, Microwave dielectric properties of $ZnNb_2O_6$-$SrTiO_3$ stacked resonators. J. Electron. Mater. **46**, 2387–2392 (2017)
17. M.H. Weng, C.T. Liauh, S.M. Lin, H.H. Wang, R.Y. Yang, Sintering behaviors, microstructure, and microwave dielectric properties of $CaTiO_3$-$LaAlO_3$ ceramics using CuO/B_2O_3 additions. Materials **12**, 4187 (2019)
18. Z.F. Fu, J.L. Ma, P. Liu, Y. Liu, Novel temperature stable $Li_2Mg_3TiO_6$-$SrTiO_3$ composite ceramics with high Q for LTCC applications. Mater. Chem. Phys. **200**, 264–269 (2017)
19. H.S. Ren, T.Y. Xie, Z.L. Wu, F. He, Y. Zhang, S.H. Jiang, X.G. Yao, H.X. Lin, Crystal structure, phase evolution and dielectric properties in the $Li_2ZnTi_3O_8$-$SrTiO_3$ system as temperature stable high-Q material. J. Alloys Compd. **797**, 18–25 (2019)
20. H.S. Ren, Z.L. Wu, F. He, Y. Zhang, X.Y. Zhao, X.G. Yao, H.X. Lin, Investigation on phase and microstructures of a temperature stable high-Q $Li_2Zn_{0.95}Sr_{0.05}Ti_3O_8$ microwave dielectric ceramic. J. Mater. Sci. **30**, 8154–8159 (2019)
21. C.L. Huang, M.H. Weng, Improved high Q value of $MgTiO_3$-$CaTiO_3$ microwave dielectric ceramics at low sintering temperature. Mater. Res. Bull. **36**, 2741–2750 (2001)
22. W.W. Cho, K. Kakimoto, H. Ohsato, High-Q microwave dielectric $SrTiO_3$-doped $MgTiO_3$ materials with near-zero temperature coefficient of resonant frequency. Jpn. J. Appl. Phys. **43**, 6221–6224 (2004)
23. P.L. Wise, I.M. Reaney, W.E. Lee, T.J. Prize, D.M. Iddles, D.S. Cannell, Structure-microwave property relations in $(Sr_xCa_{1-x})_{n+1}Ti_nO_{3n+1}$. J. Eur. Ceram. Soc. **21**, 1723–1726 (2001)
24. C.L. Pan, C.H. Shen, P.C. Chen, T.C. Tan, Characterization and dielectric behavior of a new dielectric ceramics $MgTiO_3$-$Ca_{0.8}Sr_{0.2}TiO_3$ at microwave frequencies. J. Alloys Compd. **503**, 365–369 (2010)
25. J. Zhang, Y. Luo, Z.X. Yue, L.T. Li, Temperature stability, low loss and defect relaxation of MgO-TiO_2 microwave dielectric ceramics modified by $Ca_{0.8}Sr_{0.2}TiO_3$. Ceram. Int. **44**, 141–145 (2018)
26. M.P. Seabra, V.M. Ferreira, H. Zheng, I.M. Reaney, Structure property relations in $La(Mg_{1/2}Ti_{1/2})O_3$-based solid solutions. J. Appl. Phys. **97**, 033525 (2005)

27. J. Varghese, T. Siponkoski, M. Nelo, M.T. Sebastian, H. Jantunen, Microwave dielectric properties of low-temperature sinterable α-MoO_3. J. Eur. Ceram. Soc. **38**, 1541–1547 (2018)
28. B. Ullah, W. Lei, Q.S. Cao, Z.Y. Zou, X.K. Lan, X.H. Wang, W.Z. Lu, Structure and microwave dielectric behavior of A-site-doped $Sr_{1-1.5x}Ce_xTiO_3$ ceramics system. J. Am. Ceram. Soc. **99**, 3286–3292 (2016)
29. P. Yang, Z.Q. Liu, H.B. Qi, Z.J. Peng, X.L. Fu, High-performance inductive couplers based on novel Ce^{3+} and Co^{2+} ions co-doped Ni-Zn ferrites. Ceram. Int. **45**, 13685–13691 (2019)
30. Y. Kobayashi, M. Katoh, Microwave measurement of dielectric properties of low-loss materials by the dielectric rod resonator method. IEEE Trans. Microw. Theory Technol. **33**, 586–592 (1985)
31. I.M. Reaney, D. Iddles, Microwave dielectric ceramics for resonators and filters in mobile phone networks. J. Am. Ceram. Soc. **89**, 2063–2072 (2006)
32. B. Jancar, D. Suvorov, M. Valant, G. Drazic, Characterization of $CaTiO_3$-$NdAlO_3$ dielectric ceramics. J. Eur. Ceram. Soc. **23**, 1391–1400 (2003)
33. D.W. Kim, B.W. Park, J.H. Chung, Mixture behaviour microwave dielectric properties in the low fired TiO_2-CuO system. Jpn. J. Appl. Phys. **39**, 2696–2700 (2000)
34. S.J. Penn, N.M. Alford, A. Templeton, X.R. Wang, M.S. Xu, M. Reece, K. Schrapel, Effect of porosity and grain size on the microwave dielectric properties of sintered alumina. J. Am. Ceram. Soc. **80**, 1885–1888 (1997)
35. C.F. Yang, C.C. Chan, C.M. Cheng, Y.C. Chen, 'The sintering and microwave dielectric characteristics of $MgTa_{1.5}Nb_{0.5}O_6$ ceramics. J. Eur. Ceram. Soc. **25**, 2849–2852 (2005)
36. A. Kan, H. Ogawa, H. Ohsato, Influence of microstructure on microwave dielectric properties of $ZnTa_2O_6$ ceramics with low dielectric loss. J. Alloys Compd. **337**, 303–308 (2002)
37. C.L. Huang, S.S. Liu, Characterization of extremely low loss dielectrics $(Mg_{0.95}Zn_{0.05})TiO_3$ at microwave frequency. Jpn. J. Appl. Phys. **46**, 283–285 (2007)

Publisher's Note Springer Nature remains neutral with regard to jurisdictional claims in published maps and institutional affiliations.